Transport in Porous Media (2006) 64: 15–23
DOI 10.1007/s11242-005-1396-z

The Onset of Darcy–Forchheimer Convection in Inclined Porous Layers Heated from Below

D. A. S. REES[1,⋆], A. POSTELNICU[2] and L. STORESLETTEN[3]
[1]*Department of Mechanical Engineering, University of Bath, Claverton Down, Bath BA2 7AY, U.K.*
[2]*Department of Thermal Engineering and Fluid Mechanics, Transilvania University, Brasov, 500036, Romania*
[3]*Department of Mathematics, Agder University College, Serviceboks 422, 4604 Kristiandsand, Norway*

(Received: 2 March 2005; in final form: 25 July 2005)

Abstract. It is well known that the onset of convection in an inclined porous layer heated from below takes the form of longitudinal vortices when Darcy's law is valid. In this paper we consider briefly how the onset criterion alters when form drag, as modelled by the Forchheimer terms, is significant. In general, the critical Rayleigh number increases substantially as form drag effects strengthen, but the wavenumber rises by only a small amount. This numerical study is supplemented by a brief asymptotic analysis of the case when the Forchheimer terms dominate and it is shown that the critical Rayleigh number increases in direct proportion with the form drag parameter.

Key words: convection, inclined porous layer, form drag, linear instability.

1. Introduction

Very many authors have been associated with the Darcy–Bénard problem, namely the onset and development of convection in a uniform thickness, fluid-saturated, porous layer which is heated from below. Early studies considered linearised theory and the subject has since developed to consider (i) flows at increasingly high Rayleigh numbers, (ii) the stability of such flows and (iii) the manner in which successive destabilisations take place. Additionally, the equations used to model flow and heat transfer in porous media are subject to a wide range of different extensions. Some of these include form drag effects (Forchheimer terms), no-slip effects (Brinkman terms), thermal dispersion, anisotropy, layering, variable permeability and the two-temperature model of thermal energy transport. Much of this work is summarised in the various reviews by Kimura (1998), Nield and Bejan (1999), Rees (2000), and Tyvand (2002).

⋆Author for correspondence: email: ensdasr@bath.ac.uk

It is well known that when the layer is inclined and when Darcy's law applies, then convection takes the form of longitudinal vortices if the layer is of large or unbounded spanwise extent; see Caltagirone and Bories (1985) for a detailed discussion. In view of the statements regarding extensions to Darcy's law in the above paragraph, it is surprising that there does not yet exist an analysis of the effect of form drag on convection in an inclined layer. Form drag is the additional resistance due to microscopic wake and flow separation effects, and forms an intermediate regime between viscous-dominated flow and unsteady/turbulent microscopic flow. Three recent studies exist which include form drag in the horizontal Darcy–Bénard problem. He and Georgiadis (1990) considered the combined effect of form drag, internal heating and thermal dispersion on the onset of convection and its very early development. They found that the usual pitchfork bifurcation is replaced by a pair of sharp-nosed bifurcations. Rees (1996) looked at a full weakly nonlinear stability analysis in presence of form drag only and determined how stability boundaries change as form drag effects increase. That work also confirmed the fact that form drag does not affect the onset criterion for convection since it is modelled by a nonlinear term with a no-flow basic state. Most recently Rees *et al.* (in progress) have considered hexagonal cell convection due to the presence of viscous dissipation, but part of that analysis shows that, when form drag effects increase, then hexagonal convection eventually loses its stability unconditionally and roll convection is re-established.

This short paper is concerned with the onset of vortex convection in an inclined layer in the presence of form drag. The problem differs from that of a horizontal layer since there is always a basic flow when the layer is inclined. We assume that vortices remain the favoured pattern of convection; a full proof of this is outside of the scope of the present work. Although one might suspect that there should be two free parameters to vary, namely a form drag parameter and the inclination of the layer, it is possible to combine these into one. Detailed numerical results are given for the combined effects of form drag and inclination on both the critical Rayleigh number and the associated wavenumber and these are supplemented by an asymptotic analysis for the cases where form drag dominates.

2. Governing Equations

The full nondimensional equations governing free convection in an inclined porous layer heated from below and where form drag effects cannot be neglected are

$$u_x + v_y + w_z = 0, \tag{1}$$

$$u(1 + Gq) = -p_x + R\theta \sin \alpha, \tag{2}$$

$$v(1+Gq) = -p_y + R\theta \cos\alpha, \tag{3}$$

$$w(1+Gq) = -p_z, \tag{4}$$

$$\theta_t + u\theta_x + v\theta_y + w\theta_z = \nabla^2\theta. \tag{5}$$

Here x, y and z are the streamwise, cross-stream and spanwise coordinates, respectively, and u, v and w are the corresponding fluid seepage velocities. The value q is a fluid speed given by

$$q = (u^2 + v^2 + w^2)^{1/2} \geqslant 0 \tag{6}$$

and α is the inclination of the layer from the horizontal. The variables θ and p denote dimensionless temperature and pressure, respectively. The Darcy–Rayleigh number and the form drag parameter are given by

$$R = \frac{\rho g \beta K d\, \Delta T}{\mu\kappa}, \qquad G = \frac{\tilde{K}\rho\kappa}{\mu d}, \tag{7a}$$

respectively, where ρ is a reference fluid density, g gravity, K permeability, d the depth of the layer, ΔT the temperature drop across the layer, μ the dynamic viscosity, κ the effective thermal diffusivity of the medium, and $\tilde{K}$ is a material parameter. We may quote Ergun's (1952) experimental relations to see how K and $\tilde{K}$ may vary with porosity, ϕ, and L, the length-scale associated with the pores:

$$K = \frac{L^2\phi^3}{150(1-\phi)^2}, \quad \tilde{K} = \frac{1.75L}{150(1-\phi)}. \tag{7b}$$

Therefore the parameter G could be said to vary with K since both K and $\tilde{K}$ are defined in terms of ϕ. However, we refer the reader to the detailed discussion on pages 9–12 of Nield and Bejan (1999) for further information on the modelling of the form drag term.

The boundary conditions required to complete the specification of the problem are

$$y = \pm\frac{1}{2}: \quad \theta = \mp\frac{1}{2}, \quad v = 0, \quad p_y = \mp\frac{1}{2}R\cos\alpha. \tag{8}$$

3. Linear Stability Analysis

The basic flow and temperature field are obtained by solving Equations (1)–(5) subject to (8) on assuming that all quantities are steady and dependent solely on y, and are,

$$\theta = -y, \quad p = -\frac{1}{2}(R\cos\alpha)y^2, \quad u = -\frac{2RG\sin\alpha\ y'}{1+[1+4RG\sin\alpha|y|]^{1/2}} \equiv \bar{U}(y), \tag{9}$$

which defines the quantity $\bar{U}$, the basic streamwise velocity profile.

If we now linearise Equations (1)–(5) about the solutions given in Equation (9), and assume that all disturbances are independent of both x and t we obtain

$$v_y + w_z = 0, \tag{10}$$

$$u(1+2Q) = R\theta \sin\alpha, \tag{11}$$

$$v(1+Q) = R\theta \cos\alpha - p_y, \tag{12}$$

$$w(1+Q) = -p_z, \tag{13}$$

$$\nabla^2\theta = -v. \tag{14}$$

Here the quantity Q is given by

$$Q = G|\bar{U}(y)|. \tag{15}$$

Equation (11) is now decoupled from the rest of the system, and serves solely to define the streamwise velocity in terms of the temperature. Given the form of Equation (10), we may define a streamfunction, ψ, according to

$$v = \psi_z, \qquad w = -\psi_y \tag{16}$$

and therefore Equations (10)–(14) reduce to

$$(1+Q)\nabla^2\psi + Q_y\psi_y = R\cos\alpha\ \theta_z, \tag{17}$$

$$\nabla^2\theta = -\psi_z. \tag{18}$$

We may now Fourier-decompose ψ and θ in the spanwise direction by means of the substitutions,

$$\psi = f(y)\cos kz, \qquad \theta = g(y)\sin kz, \tag{19}$$

where k is the wavenumber of the vortex, and therefore Equations (17) and (18) become

$$[(1+Q)f']' - k^2(1+Q)f = (R\cos\alpha)kg, \tag{20}$$

$$g'' - k^2 g = kf \tag{21}$$

and the corresponding boundary conditions are

$$f = g = 0 \quad \text{on } y = \pm\tfrac{1}{2}. \tag{22}$$

In Equations (20) and (21) primes denote differentiation with respect to y. As the present problem is now an eigenvalue problem for R, we may find R by applying the normalisation condition,

$$g'(-\tfrac{1}{2}) = 1. \tag{23}$$

Equations (20) and (21) have two free parameters other than α and which we will label as $\mathcal{R}$ and $\mathcal{G}$. The first, $\mathcal{R}$, is simply

$$\mathcal{R} = R \cos \alpha. \tag{24}$$

Given that Q may be written in the form

$$Q = \frac{2RG \sin \alpha |y|}{1 + [1 + 4RG \sin \alpha |y|]^{1/2}}, \tag{25}$$

we see that the second is

$$\mathcal{G} = RG \sin \alpha. \tag{26}$$

Neutral curves showing the variation of $\mathcal{R}$ with wavenumber, k, for any chosen value of $\mathcal{G}$ may be obtained using a straightforward shooting method algorithm employing, for example, the classical fourth order Runge–Kutta method after reduction to first order form. In the present case the standard manner in which a system such (20) and (21) is reduced to first order form involves Q' which has a discontinuous change in slope. Such discontinuities were avoided by defining the following four variables:

$$F_1 = f, \qquad F_2 = (1 + Q) f', \qquad F_3 = g \quad \text{and} \quad F_4 = g'. \tag{27}$$

Therefore the first order system we solved is

$$F_1' = F_2/(1 + Q), \tag{28a}$$

$$F_2' = k^2(1 + Q) F_1 + \mathcal{R} k F_3, \tag{28b}$$

$$F_3' = F_4, \tag{28c}$$

$$F_4' = k^2 F_3 + k F_1. \tag{28d}$$

As the neutral curves obtained follow the classical form with one well-defined minimum for any chosen value of $\mathcal{G}$, we have concentrated on determining the minimum value of $\mathcal{R}$ which is denoted by $\mathcal{R}_c$. The minimisation is achieved by differentiating Equations (20)–(23) with respect to k and setting $\mathrm{d}\mathcal{R}/\mathrm{d}k = 0$. Therefore we solve a 10th order system of equations with $\mathcal{R}$ and k as eigenvalues which are both dependent on the chosen value of the parameter, $\mathcal{G}$.

4. Numerical Solutions

Numerical solutions were obtained as described above and all calculations are correct to at least six significant figures. Figures 1 and 2 show the respective variations of the critical values of $\mathcal{R}$ and the minimising wavenumber, k, respectively. It was found that the value of $\mathcal{R}_c$ varies over many magnitudes, and therefore it has been presented in the form $\log_{10}(\mathcal{R}_c/4\pi^2)$.

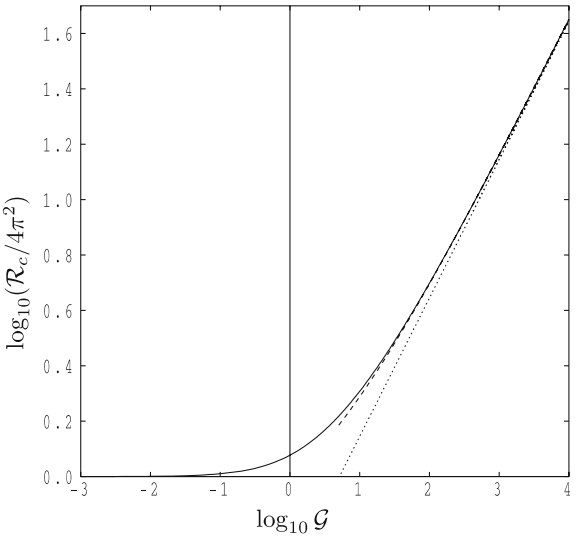

Figure 1. Variation of the critical value of $\mathcal{R}$, with $\log_{10}\mathcal{G}$. Also shown are the asymptotic forms for large values of $\mathcal{G}$: one term (short dashes) and two terms (long dashes).

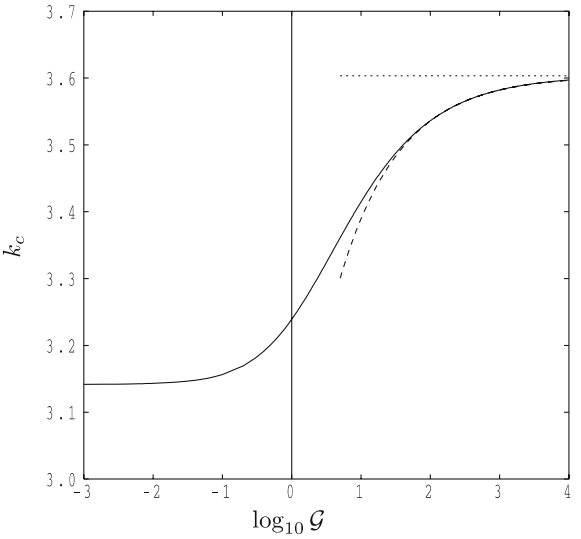

Figure 2. Variation of the critical wavenumber, k_c, with $\log_{10}\mathcal{G}$. Also shown are the asymptotic forms for large values of $\mathcal{G}$: one term (short dashes) and two terms (long dashes).

When $\mathcal{G} < 0.04$ then the critical values of $\mathcal{R}$ differ from $4\pi^2$ by less than 1%. As form drag effects increase in magnitude the value of $\mathcal{R}_c$ rises substantially and a detailed examination of the numerical solutions indicates that $\mathcal{R}_c \propto \mathcal{G}^{1/2}$ when $\mathcal{G}$ is large.

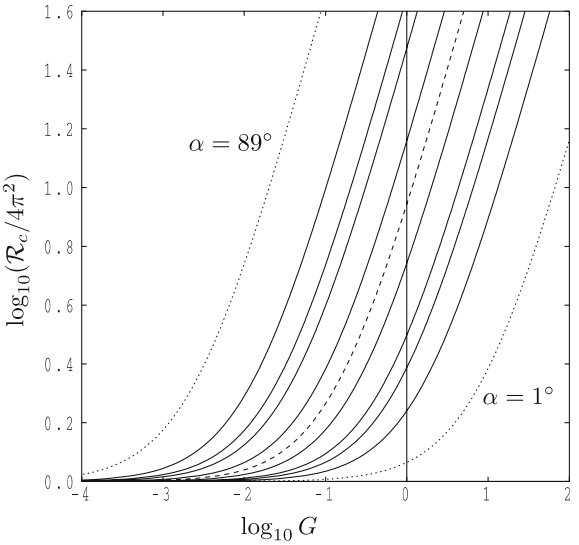

Figure 3. Variation of the critical value of $\mathcal{R}_c = R_c \cos\alpha$ with $\log_{10} G$ for the following values of α: $1°, 5°, 10°, 15°, 30°, 45°, 60°, 75°, 80°, 85°$, and $89°$. Short dashes correspond to $\alpha = 1°, 89°$ while long dashes correspond to $\alpha = 45°$. When G is small $\mathcal{R}_c$ is independent of α.

The variation of the critical wavenumber, k_c, is much less severe and is shown in Figure 2. Numerically we find that it varies between π when $\mathcal{G} = 0$ and 3.603430 as $\mathcal{G} \to \infty$. Thus the width of a convection roll reduces slightly from 1 to 0.871834. The transition between one extreme value and the other takes place over the range $0.1 \leqslant \mathcal{G} \leqslant 10,000$.

Although we have been able to compress the three governing parameters, R, G and α, into two, $\mathcal{R}$ and $\mathcal{G}$, it is not obvious how the critical Rayleigh number varies with G for a fixed value of α. Given that $\mathcal{R}_c$ is independent of α when $G = 0$, we have plotted the variation of $\mathcal{R}_c$ with G in Figure 3 for a set of values of the inclination, α, using the data shown in Figure 1. When $\alpha \ll 1$ the basic flow is relatively weak, and therefore form drag effects are relatively small. This is seen in Figure 3 by noting that, for a chosen value of $G, \mathcal{R}_c$ increases as α increases from zero. Again, a detailed examination of the associated numerical data shows that $\mathcal{R}_c \propto G$ when G is sufficiently large.

5. Asymptotic Analysis for Large Values of $\mathcal{G}$

We now turn to an analysis of the case when form drag effects dominate. Equation (25) shows that $Q \propto \mathcal{G}^{1/2}$ when $\mathcal{G} \gg 1$, and so the terms $(1 + Q)$ in Equation (20) may be replaced by Q as a first approximation. In fact $Q \sim$

$(\mathcal{G}|y|)^{1/2}$ as $\mathcal{G}\to\infty$, and therefore Equations (20) and (21) may be replaced by

$$\left(|y|^{1/2}f'\right)' - k^2|y|^{1/2}f = (\mathcal{R}/\mathcal{G}^{1/2})\,kg, \tag{29}$$

$$g'' - k^2 g = kf \tag{30}$$

and are subject to the boundary conditions (22). Practically it is easier to solve Equations (29) and (30) in the range $-\frac{1}{2}\leqslant y\leqslant 0$ and to apply symmetry conditions at $y=0$, namely that

$$f'(0) = g'(0) = 0. \tag{31}$$

A reduction to first order form following the technique introduced in Equation (27) avoids numerical difficulties due to singular derivatives.

The numerical solution of (29) yields the values

$$(\mathcal{R}/\mathcal{G}^{1/2})_c = 17.4418, \quad k_c = 3.60343. \tag{32}$$

These asymptotic values are shown in Figures 1 and 2 as the short-dashed straight lines, and these clearly show a good agreement with the fully numerical data discussed above.

The determination of a second term in the large-$\mathcal{G}$ expansion of $\mathcal{R}_c$ and k_c involves finding a local solution valid near $y=0$ where $Q\sim 1$, and using this to provide matching conditions for the equations for the second terms in the main bulk of the flow. However, the numerical data used to generate Figure 1 showed very clearly that the discrepancy between the computed value of $\mathcal{R}_c$ and the asymptotic value given in (31) is constant when $\mathcal{G}$ is sufficently large. Thus we find numerically that

$$\mathcal{R}_c \sim 17.4418\mathcal{G}^{1/2} + 21.562 \tag{33}$$

and

$$k_c \sim 3.60343 - 0.677\mathcal{G}^{-1/2}, \tag{34}$$

again we have confidence in these numerical values to the number of decimal places quoted. The variation of these values with $\mathcal{G}$ are shown in Figures 1 and 2 as long dashed lines, and we see that there is very good agreement between the computed and the asymptotic values when $\log_{10}\mathcal{G} > 1.5$.

Finally, we may use Equation (33) to find how $\mathcal{R}_c$ varies with G, rather than with $\mathcal{G}$. We obtain the expression

$$\mathcal{R}_c \sim (17.4418)^2 G\tan\alpha + 2\times 21.562. \tag{35}$$

When $G=1$ and $\alpha = 45^\circ$, Equation (35) is in error by just less than 0.4% even at such a small value of G. Thus the linear relationship between $\mathcal{R}_c$

and G, noted earlier, has been verified, and we conclude that the upwards extension of the curves given in Figure 3 may be made with a very high degree of accuracy using Equation (35).

6. Conclusion

In this short paper we have determined how the presence of form drag affects the onset criterion for the stability of convection in an inclined porous layer heated from below. When form drag effects are absent then the critical value of $\mathcal{R} = R\cos\alpha$ is independent of α. However, this independence is lost when form drag effects exist. The primary reason for this is that the strength of the basic flow now depends additionally on the magnitude of G, the form drag parameter. In general, then, we have found that the critical value of $R\cos\alpha$ increases when either the layer inclination, α, or the form drag parameter, G, increases. In particular, it was found that $R\cos\alpha \propto G$ when G is large, showing that form drag effects are very powerful in stability problems involving a basic flow.

References

Caltagirone, J. P. and Bories, S.: 1985, Solutions and stability-criteria of natural convective flow in an inclined porous layer, *J. Fluid Mech.* **155**, 267–287.

Ergun, S.: 1952, Fluid flow through packed columns, *Chem. Eng. Progr.* **48**, 89–94.

He, X. S. and Georgiadis, J. G.: 1990, Natural convection in porous media: the effect of weak disperson on bifurcation, *J. Fluid Mech.* **216**, 285–298.

Kimura, S.: 1998, Onset of oscillatory convection in a porous medium, in: D. B. Ingham and I. Pop (eds), *Transport Phenomena in Porous Media*, Pergamon, Oxford.

Nield, D. A. and Bejan, A.: 1999, *Convection in Porous Media*, 2nd edn., Springer, New York.

Rees, D. A. S.: 1996, The effect of inertia on the stability of convection in a porous layer heated from below, *J. Theor. Appl. Fluid Mech.* **1**, 154–171.

Rees, D. A. S.: 2000, The stability of Darcy–Bénard convection, in: K. Vafai (ed.), *Handbook of Porous Media*, Marcel Dekker, New York.

Tyvand, P. A.: 2002, Onset of Rayleigh–Bénard convection in porous bodies, in: D. B. Ingham and I. Pop, (eds), *Transport Phenomena in Porous Media II*, Pergamon, Oxford.